Organometallic Helicenes

Deutsche Ausgabe: DOI: 10.1002/ange.201601633
Internationale Ausgabe: DOI: 10.1002/anie.201601633

Iron Alkynyl Helicenes: Redox-Triggered Chiroptical Tuning in the IR and Near-IR Spectral Regions and Suitable for Telecommunications Applications

Chengshuo Shen, Goulc'hen Loas, Monika Srebro-Hooper, Nicolas Vanthuyne, Loïc Toupet, Olivier Cador, Frédéric Paul, Juan T. López Navarrete, Francisco J. Ramírez, Belén Nieto-Ortega, Juan Casado, Jochen Autschbach, Marc Vallet, and Jeanne Crassous**

Abstract: *The combination of a bis-alkynyl-helicene moiety with two iron centers leads to novel electroactive species displaying unprecedented redox-triggered chiroptical switching. Upon oxidation, strong changes of vibrational modes (either local or extended coupled modes) are detected by vibrational circular dichroism and Raman optical activity. Remarkably, the sign of the optical rotation at 1.54 μm (that is, at wavelengths typically used for telecommunications) changes upon oxidation while the topology and stereochemistry of the helicene remain unchanged.*

Molecular engineering combining helicenes and organometallic chemistry has recently given access to multifunctional chiral systems displaying strong chiroptical properties and other functions furnished by the metal.[1,2] This new strategy is of great interest for many optoelectronic applications.[3] An interesting class of organometallic complexes are aryl–alkynyl–iron systems which display facile electron transfer[4] enabling the redox triggering of their optical properties (for example, nonlinear optical (NLO) activity,[4c,e,5a–c] luminescence,[5d,e] absorption, and color[5f]). In this Communication, we describe unprecedented ethynyl-helicene mono- and bis-Fe^{II} complexes **2a** and **2b**, which are grafted with one or two electroactive [Fe(κ^2-dppe)(η^5-C$_5$Me$_5$)] fragments[6] (Scheme 1), and their use as efficient redox-triggered chiroptical molecular switches.[7] We demonstrate for the first time how the chiroptical properties at wavelengths typical of vibration and suitable for telecommunications applications, by means of vibrational circular dichroism (VCD),[8] resonance Raman optical activity (RROA),[9] as well as the molar rotation (MR) and electronic circular dichroism (ECD) at 1.54 μm, are influenced upon oxidation to form radical cationic species.

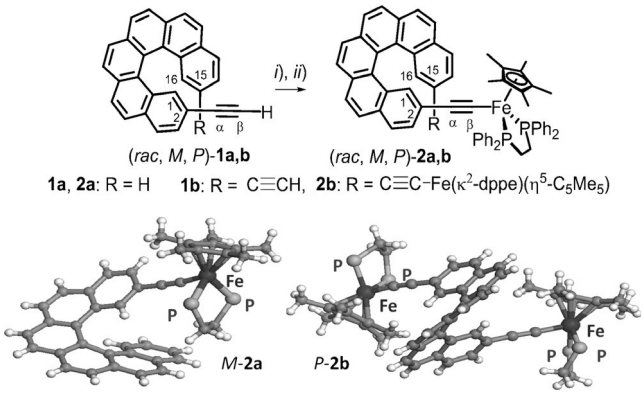

Scheme 1. Preparation of mono- and bis-Fe^{II} ethynyl[6]helicene complexes **2a**,**b** from mono- and bis-ethynyl[6]helicenes **1a**,**b**. i) [Fe(κ^2-dppe)(η^5-C$_5$Me$_5$)Cl] (**3**-Cl), MeOH, THF, NaPF$_6$; ii) THF, ^{t}BuOK. X-ray crystal structures of enantiopure *M*-**2a** and racemic **2b** (*P* enantiomer shown).[16] dppe = 1,2-bis(diphenylphosphino)ethane. The Ph groups on the dppe ligand are omitted for clarity.

The helicene-based mono- and bis-Fe^{II} complexes (*rac*,*M*,*P*)-**2a**,**b** were prepared as air-stable red solids in good yields (51–77%) from ethynyl[6]helicene ligands (*rac*,*M*,*P*)-**1a**,**b**[2e,g] and the iron salt **3**-Cl[6a] (Scheme 1). The synthesis proceeds via the formation of cationic iron vinylidene intermediates followed by their deprotonation to form the neutral complexes **2a**,**b**.[6] Full characterization is detailed in the Supporting Information.

M-**2a** and (±)-**2b** crystallized in the $P2_1$ and $P\bar{1}$ space groups, respectively. Their X-ray structures (Scheme 1; see also the Supporting Information) show regular metric data for the piano-stool-like iron fragment (typical lengths for the Fe–C$_\beta$, C$_\alpha$≡C$_\beta$, and C$_\alpha$–C$_2$ bonds circa 1.89, 1.22–1.23, and 1.42–

[*] Dr. C. Shen, Dr. G. Loas, Dr. L. Toupet, Dr. O. Cador, Dr. F. Paul, Prof. M. Vallet, Dr. J. Crassous
Institut des Sciences Chimiques de Rennes UMR 6226
Institut de Physique de Rennes
UMR 6251, CNRS Université de Rennes 1
Campus de Beaulieu, 35042 Rennes Cedex (France)
E-mail: jeanne.crassous@univ-rennes1.fr
Dr. M. Srebro-Hooper
Faculty of Chemistry, Jagiellonian University
R. Ingardena 3, 30-060 Krakow (Poland)
Dr. N. Vanthuyne
Aix Marseille Université, Centrale Marseille
CNRS, iSm2 UMR 7313, 13397 Marseille (France)
Prof. J. T. López Navarrete, Prof. F. J. Ramírez, Dr. B. Nieto-Ortega, Prof. J. Casado
Department of Physical Chemistry, University of Malaga
Campus de Teatinos s/n, Malaga 29071 (Spain)
Prof. J. Autschbach
Department of Chemistry
University at Buffalo, State University of New York
Buffalo, NY 14260 (USA)
E-mail: jochena@buffalo.edu
Supporting information and the ORCID identification number(s) for the author(s) of this article can be found under http://dx.doi.org/10.1002/anie.201601633.

1.43 Å, respectively),[6] and classical helical angles for the [6]helicenic ligands (53.1–60.5°).[2] The linearity of the ethynyl fragments ensures an efficient π-conjugation between the helicene and the iron centers (angles Fe-C_β-C_α = 173.7°, C_β-C_α-C_2 = 175.0°).

The chiroptical properties upon attachment of one or two electroactive Fe moieties (by way of fragment **3**) to a helicene-alkynyl moiety are strongly modified. For instance, the ECD spectrum of *P*-**2b** shows typical helicene bands, that is, an intense negative band at $\lambda = 300$ nm ($\Delta\varepsilon = -125\,\text{M}^{-1}\text{cm}^{-1}$) and strong positive bands at $\lambda = 337$ nm ($\Delta\varepsilon = +110\,\text{M}^{-1}\text{cm}^{-1}$) and 386 nm ($\Delta\varepsilon = +78\,\text{M}^{-1}\text{cm}^{-1}$; Figure 1a). An additional

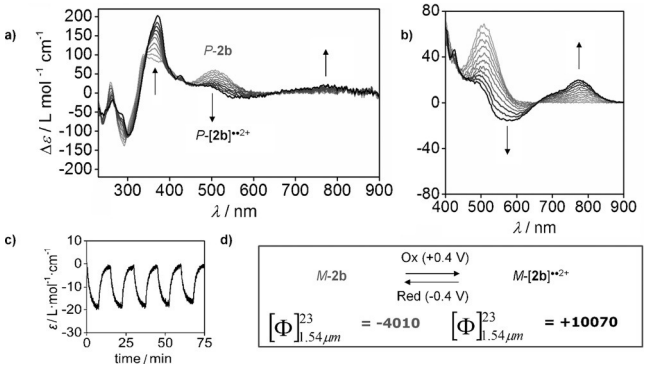

Figure 1. a, b) Oxidation of *P*-**2b** detected by ECD from the UV to the NIR region (a) and in the $\lambda = 400$–900 nm region (b). c) Redox chiroptical switching of *M*-**2b**↔[*M*-**2b**]••2+ monitored by ECD at $\lambda = 767$ nm (at ±0.4 V versus a Pt pseudopotential reference electrode). d) Modification of the molar rotation values at wavelengths typically used for telecommunications (1.54 μm, CH_2Cl_2, C = 10 mg mL^{-1}). ε = molar extinction coefficient; $[\Phi]^{23}_{1.54\,\mu m}$ values refer to the molar rotation in ° cm^2 dmol^{-1} measured at 1.54 μm at 23°C.

intense broad positive band at $\lambda = 506$ nm ($\Delta\varepsilon = +68\,\text{M}^{-1}\text{cm}^{-1}$) corresponds to the HOMO→LUMO transition which leads to charge transfer from fragment **3** to the helicene, as determined by time-dependent density functional theory (TDDFT;[10] Figure 2, bottom; see also the Supporting Information). The HOMO of **2b** mainly extends over **3**, while the LUMO is a helicene π* orbital.

Cyclic voltammetry shows one reversible oxidation wave at −0.144 V (versus the saturated calomel electrode (SCE)) for **2a** and two waves at −0.180 and −0.089 V for **2b** (see the Supporting Information). The one- (**2a**) and two-electron (**2b**) oxidation processes were monitored by ECD[2c,e] either chemically with iodine or spectroelectrochemically ($C_2H_4Cl_2$/NBu_4PF_6, 0.2 M). For example, upon oxidation of *P*-**2b** to *P*-[**2b**]••2+ there is 1) a strong increase of the positive ECD band around $\lambda = 350$ nm ($\Delta(\Delta\varepsilon) > +100\,\text{M}^{-1}\text{cm}^{-1}$ at $\lambda = 372$ nm), 2) a strong decrease of the positive band between $\lambda = 530$–650 nm with the appearance of a negative band, and 3) the appearance of a broad band in the Vis/NIR region ($\lambda = 670$–900 nm, $\Delta(\Delta\varepsilon) \approx +20\,\text{M}^{-1}\text{cm}^{-1}$ at $\lambda = 767$ nm; see Figure 1). Interestingly, an ECD band of the *M*-[**2b**]••2+ oxidized species was also detected in the NIR region ($\lambda = 1540$ nm; $\Delta\varepsilon = -0.09\,\text{M}^{-1}\text{cm}^{-1}$). These ECD oxidation-induced changes are well reproduced by calculations (Figure 2; see the Supporting

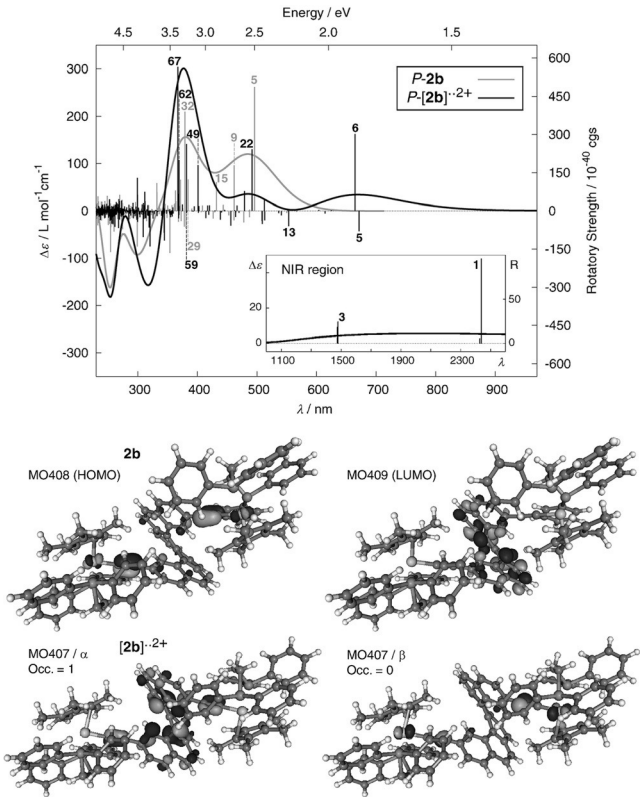

Figure 2. Top: Simulated B3LYP/SV(P) ECD spectra of *P*-**2b** (gray) and *P*-^{3}[**2b**]••2+ (black). Calculated excitation energies and rotatory strengths indicated as "stick" spectra. Numbered excitations were analyzed in detail (see the Supporting Information). Inset: NIR ECD of *P*-^{3}[**2b**]••2+. Bottom: Isosurfaces (0.04 a.u.) of frontier MOs of **2b**/^{3}[**2b**]••2+.

Information for the molecular orbital analysis). Upon reduction, the spectral changes reversed and [**2b**]••2+ changed back to **2b**. The reversible redox modifications of the ECD spectra mean that **2a**,**b** behave as chiroptical switches (Figure 1c; see also the Supporting Information).[2c,e,3b,7]

Relative to their organic precursors, **2a**,**b** display molar rotations (MRs) (D line, 589 nm) that are strongly enhanced by the proximity to an electronic resonance (for example, *P*-**2b** (*P*-**1b**[2c,e]): $[\Phi]^{23}_D = +79\,700°$ (+20 000°) cm^2 dmol^{-1} (calculated 83 844 (22 230))). Upon oxidation, the MRs of **2a**,**b** undergo a strong (four to tenfold) decrease in magnitude. This can be rationalized by the corresponding changes in the ECD spectrum around $\lambda = 500$ nm, which have a compensating effect on the optical rotation (for example, *P*-**2b**→*P*-[**2b**]••2+,2I$^-$: $[\Phi]^{23}_D = +79\,700 \rightarrow +8990°$ cm^2 dmol^{-1}; see the Supporting Information).

Materials which are stimuli-responsive at wavelengths typically used for telecommunications may be of great interest for transmitting encoded information.[11] Interestingly, using an in-house-developed polarimeter, molar rotations of −2370 and −4010° cm^2 dmol^{-1} for *M*-**2a** and *M*-**2b**, respectively, were measured at 1.54 μm, that is, providing the transmitted light with a chiroptical tag, which inverts its sign upon oxidation processes *M*-**2a**→*M*-[**2a**]•+ (see the Supporting Information) and *M*-**2b**→*M*-[**2b**]••2+ (Figure 1d). These drastic changes illustrate well the potential to efficiently tune

or even reverse chiroptical properties at wavelengths suitable for telecommunications while maintaining the integrity of the helical backbone. They can be rationalized by the presence of ECD-active electronic excitations around 1.54 μm for the oxidized species, which causes anomalous optical rotation (OR) dispersion that can change the sign of the OR.[10b,12] This case therefore constitutes a new type of redox-triggered chiroptical switch using a clear output tag at 1.54 μm, that is, outside the more common wavelength regions.

Apart from ECD and optical rotation, vibrational optical activity, that is, VCD and ROA,[12] provide additional molecular-level information related to the chirality and redox switching. Figure 3 shows the IR and VCD spectra of

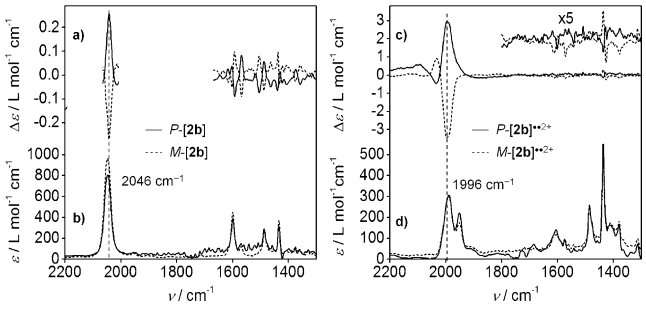

Figure 3. Experimental VCD spectra of *M*- and *P*-**2b** (a) and *M*- and *P*-[**2b**]$^{\bullet 2+}$ (c), along with the corresponding IR spectra of *M*- and *P*-**2b** (b) and *M*- and *P*-[**2b**]$^{\bullet 2+}$ (d; CD_2Cl_2, $C \approx 3\times10^{-3}$ M).

enantiopure complexes *M*- and *P*-**2b** and *M*- and *P*-[**2b**]$^{\bullet 2+}$. Several interesting spectroscopic features are found, notably: 1) a strong IR- and VCD-active mode at 2046 cm^{-1} corresponding to the C≡C stretch, with a positive VCD sign; 2) two negative–positive signatures at 1595–1566 and 1500–1485 cm^{-1} belonging to C=C stretches coupled with CCH bending (see the Supporting Information).[2e] Upon chemical oxidation with iodine, the C≡C stretching band appears split and at lower wavenumbers (1996 and 2032 cm^{-1}), probably due to Fermi coupling,[6b] with a negative–positive VCD pattern. The wavenumber decrease is probably due to delocalization of the hole into the acetylene spacer which thus acquires some cumulenic C=C=Fe character. More interestingly, a 30-fold increase of the dissymmetry factor is observed upon oxidation ($g = \Delta\varepsilon/\varepsilon$ from 3×10^{-4} to 10^{-2}). The strong enhancement supports the presence of electron spin density within the C≡C moiety which may give rise to stronger magnetic transition dipole moments within the vibrational transitions. Indeed, the paramagnetic character of radical cationic species *P*-[**2a**]$^{\bullet+}$ and *P*-[**2b**]$^{\bullet 2+}$ is clearly evidenced by susceptibility and ^{1}H NMR measurements (see the Supporting Information) and calculations show how spin density delocalizes from the metal into the helical backbone (Figure S40). Low-lying electronic states can also account for such an enhancement.[13] To our knowledge this is the first time that such an increase is observed upon modifying the electron density of a helicenic species. Note that other modifications are observed in the 1600–1450 cm^{-1} region, and very similar trends were obtained for the monometallic complex **2a** (see the Supporting Information).

To date, (resonance) Raman and Raman optical activity (ROA) spectroscopy,[12] which are complementary techniques to IR and VCD, are far less utilized in helicene chemistry and in coordination chemistry.[9] For **2a**,**b** (Figure 4; see also the

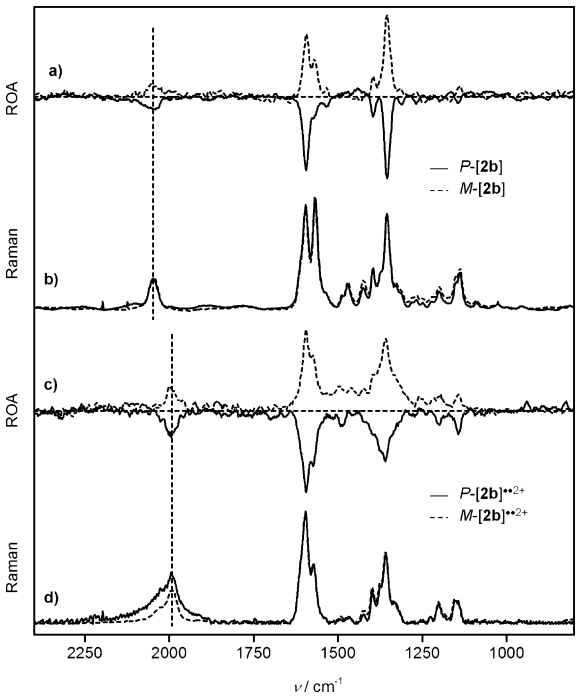

Figure 4. Experimental ROA spectra of *M*- and *P*-**2b** (a) and *M*- and *P*-[**2b**]$^{\cdot 2+}$ (c). Experimental Raman spectra of *M*- and *P*-**2b** (b) and *M*- and *P*-[**2b**]$^{\cdot 2+}$ (d); (CH_2Cl_2, $C \approx 3\times10^{-3}$ M).

Supporting Information), three modes were found to be strongly Raman active: the G-mode (graphene-like CC stretching mode) at 1594 cm^{-1}, the D-mode (diamond-like CC breathing mode) at 1355 cm^{-1} and the C≡C stretching mode at 2046 cm^{-1}.[9a,14] Noteworthily, all ROA bands display the same sign, that is, negative for the *P* enantiomers and all positive for the *M* enantiomers. The experimental wavelength used for measurements ($\lambda = 532$ nm) coincides with an electronic absorption band of the spectra for both **2a** and **2b**, which implies that what we observe is resonant ROA (RROA).[12,15] The RROA signals are: 1) monosignate; 2) of the opposite sign to that of the ECD band at the $\lambda = 532$ nm resonant Raman excitation; and 3) the dissymmetry factors *g* of the ECD versus those of the RROA overall follow a $g(\mathrm{RROA}) = -g(\mathrm{ECD})/2$ relationship. For instance, in *P*-[**2b**]$^{\bullet 2+}$ the RROA bands have $g = -0.002$ whereas the corresponding value for the ECD is $g = +0.004$. These features are in agreement with the ROA expected for a single electronic state resonance situation.[15] Here again, iodine oxidation provokes significant modifications of the Raman and ROA spectra, and complementarily to VCD shows that not only the C≡C stretching mode is affected (changing from 2046 to 1988 cm^{-1}) but also the G- and D-modes (Figure 4; see also the Supporting Information),

confirming the involvement and alteration of the π-conjugated structure within the helicene core. To our knowledge, this is the first time where ROA is used for examining modifications upon redox changes. This technique may be useful for studying other chiral systems, such as chiral fullerenes or carbon nanotubes.[14]

In summary, we have shown that while keeping the integrity of their structure, organometallic helicenes can invert their optical rotation at 1.54 μm upon oxidation. Furthermore, VCD and ROA spectroscopy provide a molecular level description of the effect of redox neutral→cation switch at the origin of the several tenfold magnitude increase along with frequency shifts. The switching described in this study demonstrates the possibility to select the dichroic signal of an incoming circularly polarized light beam at wavelengths typical of vibration and suitable for telecommunications applications. At present, light encoding processes for the treatment of optical information are achieved by ultrafast optical switching. Future research will need to focus on improving the speed of the switching processes in solid-state device prototypes.

Acknowledgements

This work was supported by the ANR (12-BS07-0004-METALHEL-01), the French Ministry of Research, and the CNRS (project DIL "CARIM"). M.S.-H. acknowledges the FNP Homing Plus programme cofinanced by EU funds and a Ministry of Science and Higher Education in Poland scholarship. J.A. acknowledges an NSF Grant (CHE-1265833) and the Center for Computational Research in Buffalo for computational support.

Keywords: circular dichroism · helicenes · iron · optical rotation · Raman optical activity

How to cite: *Angew. Chem. Int. Ed.* **2016**, *55*, 8062–8066
Angew. Chem. **2016**, *128*, 8194–8198

[1] For selected reviews on helicene properties, see: a) Y. Shen, C.-F. Chen, *Chem. Rev.* **2012**, *112*, 1463; b) M. Gingras, *Chem. Soc. Rev.* **2013**, *42*, 1051; c) N. Saleh, C. Shen, J. Crassous, *Chem. Sci.* **2014**, *5*, 3680.

[2] a) L. Norel, M. Rudolph, N. Vanthuyne, J. A. G. Williams, C. Lescop, C. Roussel, J. Autschbach, J. Crassous, R. Réau, *Angew. Chem. Int. Ed.* **2010**, *49*, 99; *Angew. Chem.* **2010**, *122*, 103; b) E. Anger, M. Rudolph, C. Shen, N. Vanthuyne, L. Toupet, C. Roussel, J. Autschbach, J. Crassous, R. Réau, *J. Am. Chem. Soc.* **2011**, *133*, 3800; c) E. Anger, M. Srebro, N. Vanthuyne, L. Toupet, S. Rigaut, C. Roussel, J. Autschbach, J. Crassous, R. Réau, *J. Am. Chem. Soc.* **2012**, *134*, 15628; d) E. Anger, M. Srebro, N. Vanthuyne, C. Roussel, L. Toupet, J. Autschbach, R. Réau, J. Crassous, *Chem. Commun.* **2014**, *50*, 2854; e) M. Srebro, E. Anger, B. Moore II, N. Vanthuyne, C. Roussel, R. Réau, J. Autschbach, J. Crassous, *Chem. Eur. J.* **2015**, *21*, 17100.

[3] a) Y. Yang, R. C. da Costa, M. J. Fuchter, A. J. Campbell, *Nat. Photonics* **2013**, *7*, 634; b) D. Schweinfurth, M. Zalibera, M. Kathan, C. Shen, M. Mazzolini, N. Trapp, J. Crassous, G. Gescheidt, F. Diederich, *J. Am. Chem. Soc.* **2014**, *136*, 13045; c) R. A. van Delden, M. K. J. ter Wiel, M. M. Pollard, J. Vicario, N. Koumura, B. L. Feringa, *Nature* **2005**, *437*, 1337; d) T. R. Kelly, H. De Silva, R. A. Silva, *Nature* **1999**, *401*, 150; e) T. Verbiest, S. Van Elshocht, M. Kauranen, L. Hellemans, J. Snauwaert, C. Nuckolls, T. J. Katz, A. Persoons, *Science* **1998**, *282*, 913; f) L. Pospisil, L. Bednarova, P. Stepanek, P. Slavicek, J. Vavra, M. Hromadova, H. Dlouha, J. Tarabek, F. Teply, *J. Am. Chem. Soc.* **2014**, *136*, 10826.

[4] a) F. Paul, C. Lapinte, *Coord. Chem. Rev.* **1998**, *178*, 431; b) P. Aguirre-Etcheverry, D. O'Hare, *Chem. Rev.* **2010**, *110*, 4839; c) G. Grelaud, M. P. Cifuentes, F. Paul, M. G. Humphrey, *J. Organomet. Chem.* **2014**, *751*, 181; d) J.-F. Halet, C. Lapinte, *Coord. Chem. Rev.* **2013**, *257*, 1584; e) B. J. Coe, *Coord. Chem. Rev.* **2013**, *257*, 1438.

[5] a) M. Samoc, N. Gauthier, M. P. Cifuentes, F. Paul, C. Lapinte, M. G. Humphrey, *Angew. Chem. Int. Ed.* **2006**, *45*, 7376; *Angew. Chem.* **2006**, *118*, 7536; b) C. E. Powell, M. P. Cifuentes, J. P. Morrall, R. Stranger, M. G. Humphrey, M. Samoc, B. Luther-Davies, G. A. Heath, *J. Am. Chem. Soc.* **2003**, *125*, 602; c) K. A. Green, M. P. Cifuentes, T. C. Corkery, M. Samoc, M. G. Humphrey, *Angew. Chem. Int. Ed.* **2009**, *48*, 7867; *Angew. Chem.* **2009**, *121*, 8007; d) E. Di Piazza, L. Norel, K. Costuas, A. Bourdolle, O. Maury, S. Rigaut, *J. Am. Chem. Soc.* **2011**, *133*, 6174; e) M. Murai, M. Sugimoto, M. Akita, *Dalton Trans.* **2013**, *42*, 16108; f) Y. Tanaka, T. Ishisaka, A. Inagaki, T. Koike, C. Lapinte, M. Akita, *Chem. Eur. J.* **2010**, *16*, 4762.

[6] a) C. Roger, P. Hamon, L. Toupet, H. Rabaa, J.-Y. Saillard, J.-R. Hamon, C. Lapinte, *Organometallics* **1991**, *10*, 1045; b) F. Paul, J.-Y. Mevellec, C. Lapinte, *Dalton Trans.* **2002**, 1783; c) F. Paul, A. Bondon, G. da Costa, F. Malvolti, S. Sinbandhit, O. Cador, K. Costuas, L. Toupet, M.-L. Boillot, *Inorg. Chem.* **2009**, *48*, 10608; d) K. Costuas, F. Paul, L. Toupet, J.-F. Halet, C. Lapinte, *Organometallics* **2004**, *23*, 2053.

[7] See H. Isla, J. Crassous, *C. R. Chim.* **2016**, *19*, 39, and references therein.

[8] a) T. Bürgi, A. Urakawa, B. Behzadi, K.-H. Ernst, A. Baiker, *New J. Chem.* **2004**, *28*, 332; b) S. Abbate, F. Lebon, G. Longhi, F. Fontana, T. Caronna, D. A. Lightner, *Phys. Chem. Chem. Phys.* **2009**, *11*, 9039; c) S. Abbate, G. Longhi, F. Lebon, E. Castiglioni, S. Superchi, L. Pisani, F. Fontana, F. Torricelli, T. Caronna, C. Villani, R. Sabia, M. Tommasini, A. Lucotti, D. Mendola, A. Mele, D. A. Lightner, *J. Phys. Chem. C* **2014**, *118*, 1682; d) T. B. Freedman, X. Cao, A. Rajca, H. Wang, L. A. Nafie, *J. Phys. Chem. A* **2003**, *107*, 7692; e) F. Torricelli, J. Bosson, C. Besnard, M. Chekini, T. Bürgi, J. Lacour, *Angew. Chem. Int. Ed.* **2013**, *52*, 1796; *Angew. Chem.* **2013**, *125*, 1840; f) V. P. Nicu, J. Neugebauer, S. K. Wolff, E. J. Baerends, *Theor. Chem. Acc.* **2008**, *119*, 245; g) V. Liégeois, B. Champagne, *J. Comput. Chem.* **2009**, *30*, 1261.

[9] For experimental ROA of helicenes, see: a) C. Johannessen, E. W. Blanch, C. Villani, S. Abbate, G. Longhi, N. R. Agarwal, M. Tommasini, D. A. Lightner, *J. Phys. Chem. B* **2013**, *117*, 2221; For theoretical ROA of helicenes, see: b) V. Liegeois, B. Champagne, *Theor. Chem. Acc.* **2012**, *131*, 1284; c) M. Tommasini, G. Longhi, G. Mazzeo, S. Abbate, B. Nieto-Ortega, F. J. Ramírez, J. Casado, J. T. L. Navarrete, *J. Chem. Theory Comput.* **2014**, *10*, 5520; d) S. Yamamoto, P. Bour, *Angew. Chem. Int. Ed.* **2012**, *51*, 11058; *Angew. Chem.* **2012**, *124*, 11220.

[10] a) J. Autschbach, *Chirality* **2009**, *21*, E116; b) J. Autschbach, L. Nitsch-Velasquez, M. Rudolph, *Top. Curr. Chem.* **2011**, *298*, 1.

[11] G. P. Agrawal, *Fiber-optic Communication Systems*, 4th ed., Wiley, Hoboken, **2010**.

[12] a) L. D. Barron, *Molecular Light Scattering and Optical Activity*, 2nd ed., Cambridge University Press, Cambridge, **2009**; b) L. A. Nafie, *Vibrational Optical Activity: Principles and Applications*, Wiley, Hoboken, **2011**.

[13] a) Y. He, X. Cao, L. A. Nafie, T. B. Freedman, *J. Am. Chem. Soc.* **2001**, *123*, 11320; b) S. R. Domingos, A. Huerta-Viga, L. Baij, S. Amirjalayer, D. A. E. Dunnebier, A. J. C. Walters, M. Finger,

L. A. Nafie, B. de Bruin, W. J. Buma, S. Woutersen, *J. Am. Chem. Soc.* **2014**, *136*, 3530, and references therein.

[14] a) E. Di Donato, M. Tommasini, G. Fustella, L. Brambilla, C. Castiglioni, G. Zerbi, C. D. Simpson, K. Mullen, F. Negri, *Chem. Phys.* **2004**, *301*, 81; b) C. Castiglioni, M. Tommasini, G. Zerbi, *Philos. Trans. R. Soc. London Ser. A* **2004**, *362*, 2425; c) M. Tommasini, C. Castiglioni, G. Zerbi, *Phys. Chem. Chem. Phys.* **2009**, *11*, 10185; d) A. C. Grimsdale, K. Mullen, *Angew. Chem. Int. Ed.* **2005**, *44*, 5592; *Angew. Chem.* **2005**, *117*, 5732.

[15] a) L. A. Nafie, *Chem. Phys.* **1996**, *205*, 309; b) M. Vargek, T. B. Freedman, E. Lee, L. A. Nafie, *Chem. Phys. Lett.* **1998**, *287*, 359; c) L. Jensen, J. Autschbach, M. Krykunov, G. C. Schatz, *J. Chem. Phys.* **2007**, *127*, 134101.

[16] CCDC 941881 and 945457 contain the supplementary crystallographic data for this paper. These data are provided free of charge by The Cambridge Crystallographic Data Centre.

Received: February 16, 2016
Published online: May 19, 2016

